HHS Public Access

Author manuscript

Nat Neurosci. Author manuscript; available in PMC 2013 February 20.

Published in final edited form as:

Nat Neurosci. 2009 November ; 12(11): 1444–1449. doi:10.1038/nn.2402.

Basal Forebrain Activation Enhances Cortical Coding of Natural Scenes

Michael Goard and **Yang Dan**[+]

Howard Hughes Medical Institute, Division of Neurobiology, Department of Molecular and Cell Biology, Helen Wills Institute of Neuroscience, University of California, Berkeley, CA 94720

Abstract

The nucleus basalis (NB) of the basal forebrain is an essential component of the neuromodulatory system controlling the behavioral state of an animal, and it is thought to play key roles in regulating arousal and attention. However, the effect of NB activation on sensory processing remains poorly understood. Using polytrode recording in rat visual cortex, we show that NB stimulation causes prominent decorrelation between neurons and marked improvement in the reliability of neuronal responses to natural scenes. The decorrelation depends on local activation of cortical muscarinic acetylcholine receptors, while the increased reliability involves distributed neural circuits, as evidenced by NB-induced changes in thalamic responses. Further analysis showed that the decorrelation and increased reliability improve cortical representation of natural stimuli in a complementary manner. Thus, the basal forebrain neuromodulatory circuit, which is known to be activated during aroused and attentive states, acts through both local and distributed mechanisms to improve sensory coding.

Neuromodulatory circuits are essential for regulating the behavioral state of an animal[1–4]. In particular, the basal forebrain cholinergic system originating from the nucleus basalis (NB) projects diffusely throughout the neocortex[5], and it is implicated in vital brain functions such as arousal, attention[6–8], and experience-dependent cortical plasticity[9–11]. The cholinergic neurons in NB are active during waking and REM sleep but not during slow wave sleep[12,13], and recent studies in awake animals have shown that NB activity varies in a task-dependent manner[14,15]. Since sensory perception can be markedly enhanced by arousal and attention, the state-dependent NB activation suggests that the basal forebrain circuit may play a significant role in dynamic modulation of sensory processing. However, the causal relationship between NB activation and enhanced sensory processing has not yet been demonstrated.

Sensory processing in the cortex is known to be affected by the intrinsic dynamics of the cortical network[16–20]. Since neuromodulators such as acetylcholine (ACh) can alter neuronal excitability[21–23] and synaptic efficacy[24–27], they may rapidly regulate circuit dynamics[21,28] and sensory processing[29]. Indeed, local iontophoretic application of ACh has

[+]To whom the correspondence should be addressed: Yang Dan: Phone: 510-643-2833, ydan@berkeley.edu.

Author Contributions: M.G. conducted all experiments; M.G. and Y.D. designed the experiments and wrote the manuscript.

been shown to affect the contrast gain[30], orientation and direction selectivity[31-34], and attentional modulation[35] of visual cortical neurons. However, these local changes may not fully reflect the effects of NB activation, as the NB projection to the cortex is highly diffuse, and its activation is known to affect the global pattern of brain activity[21,36]. Thus, to understand the role of the basal forebrain neuromodulatory circuit in sensory perception, it is important to test the effect of NB activation on the sensory responses of a population of cortical neurons.

In this study, we used multielectrode recording in rat visual cortex to demonstrate two prominent effects of NB activation on cortical responses to natural stimuli. Brief NB stimulation caused a strong decorrelation between cortical neurons and a marked increase in the reliability of visually evoked responses. Furthermore, we showed that these two effects are mediated by distinct mechanisms and that they contribute to improved visual coding in a complementary manner. These findings provide a direct demonstration that a neuromodulatory circuit can dynamically regulate cortical coding of sensory inputs.

Results

We stimulated the NB of urethane-anesthetized rats with a bipolar electrode while recording from ipsilateral V1 with a silicon polytrode spanning the cortical depth[37] (Fig. 1a). The NB location was identified during the experiment by measuring the change in power spectrum of the interhemispheric electroencephalogram (EEG, Supplementary Fig. 1 online)[21,36] induced by a stimulus train (500 ms, 100 Hz) and confirmed by acetylcholinesterase staining[38] in a subset of experiments (Fig. 1b,c).

In the absence of visual input, each NB stimulus train caused a marked change in the power spectrum of V1 local field potential (LFP), with an increase in power at 10 to 100 Hz (particularly in the gamma band, 30 to 50 Hz) and a decrease at low frequencies (<10 Hz) (Fig. 1d). As quantified by the power ratio (LFP power at 10 to 100 Hz divided by that at 1 to 10 Hz), this effect on spontaneous cortical activity lasted for5 to 10 s (Fig. 1e). To characterize the effect of NB stimulation on visually driven responses, we presented each natural movie to the contralateral eye both before (control) and immediately after NB stimulation (5 s per movie, 30 repeats per condition) and recorded multiunit activity from 27 channels of the polytrode (see Online Methods). In the control condition, the multiunit activity was highly correlated among the channels throughout the cortical column, but poorly time-locked to the stimulus (Fig. 2). However, following NB stimulation, the activity was less correlated among channels but appeared more time-locked to the movie.

NB stimulation reduces correlation, increases reliability

We then examined these effects at the level of single units, each sorted from the signals recorded at 2 to 4 nearby channels (see Online Methods). As shown by the spike trains of multiple simultaneously recorded single units in three example experiments (Fig. 3a; each neuron indicated by a different color), NB stimulation caused a conspicuous decorrelation between cells in response to natural movies. To quantify the decorrelation for each cell, we computed the average Pearson correlation coefficient (CC) between its response and the responses of all other cells in the same recording. We found that NB stimulation caused a

strong reduction of between-cell CC across 166 neurons from 19 experiments (Fig. 3b; $P < 10^{-28}$, Wilcoxon signed-rank test).

We also examined the effect of NB stimulation on the response reliability of each neuron by analyzing the single unit responses to 30 repeats of a natural movie (Fig. 4a; each neuron indicated by a different color). In the control condition, there was considerable variability across trials, but NB stimulation markedly improved the reliability of the responses. To quantify the reliability for each cell, we computed the Pearson CC of its responses between each pair of repeats and averaged the CCs over all pairwise combinations. Across the 166 neurons recorded in 19 experiments, NB stimulation consistently increased the response reliability (Fig. 4b; $P < 10^{-28}$, Wilcoxon signed-rank test). Note that in the experiments in which electrical stimulation of NB did not elicit significant desynchronization of cortical EEG ($n = 4$, excluded from the above analyses), neither decreased correlation nor increased reliability was observed (Supplementary Table 1 online), suggesting that these effects rely on activation of the same set of neurons that are also responsible for EEG desynchronization.

When the above analyses were performed for each cortical layer separately, we observed significant decreases in between-cell correlation and increases in response reliability in all layers (Supplementary Fig. 2a,b online). In contrast, the effect of NB stimulation on cortical firing rate varied across layers: it caused modest increases in layers 4, 5, and 6, but a decrease in layer 2/3 (Supplementary Fig. 2c online). To ensure that the changes in between-cell correlation and response reliability were not due to NB-induced changes in cortical firing rate, we equalized the firing rates of each neuron before and after NB stimulation by randomly deleting spikes from the spike train with higher rate (Supplementary Fig. 3a,c online). Both effects remained highly significant after spike rate equalization (Supplementary Fig. 3b,d online; $P < 10^{-22}$, Wilcoxon signed-rank test, n = 166 neurons from 19 experiments). Furthermore, these changes could not be accounted for by the effect of repeated visual stimulus presentation, since the blocks of control and NB trials were interleaved in the experiment (see Online Methods), and the differences in reliability and between-cell CC across blocks were much smaller than those between the control and NB conditions (Supplementary Fig. 4 online).

We also tested whether the NB-induced changes in the cortical responses to natural scenes were accompanied by changes in the receptive field properties. Both ON and OFF receptive fields of each neuron were measured with sparse noise stimuli before and after NB stimulation (Supplementary Fig. 5a,b online). We found no significant change in receptive field size [$P = 0.07$ (ON) and $P = 0.41$ (OFF), $n = 38$ from 5 experiments, Supplementary Fig. 5c online], but a significant increase in the ratio of the peak amplitude to baseline noise [$P < 10^{-4}$ (ON) and $P < 10^{-4}$ (OFF), $n = 38$ from 5 experiments, Supplementary Fig. 5d online]. This is likely to reflect NB-induced improvement in response reliability that is also observed with natural stimuli. Previous studies showed that cortical iontophoresis of ACh could induce changes in orientation tuning and direction selectivity, although the observed effects were variable between cells and across studies[31–34]. Using drifting gratings to measure the orientation tuning of cortical neurons before and after NB stimulation (Supplementary Fig. 6a,b online), we found no significant change in orientation tuning

width ($P = 0.78$, $n = 35$ from 10 experiments, Supplementary Fig. 6c online) or direction selectivity ($P = 0.20$, $n = 35$ from 10 experiments, Supplementary Fig. 6d online) at the population level. Thus, instead of systematic alteration of receptive field properties, the most consistent effect of NB stimulation across cortical neurons was the improvement of visual response reliability.

NB-induced decorrelation depends on cortical mAChRs

Previous studies showed that the change in EEG pattern induced by NB activation depends on cortical muscarinic acetylcholine receptors (mAChRs)[21]. We thus tested the role of mAChRs in NB-induced changes in cortical responses by applying atropine sulfate, a selective mAChR antagonist, to the recording area via either intracortical injection with a micropipette (100 μM) or local application to the cortical surface (1 mM; see Online Methods). As shown in an example multiunit recording (Fig. 5a), atropine application greatly reduced the degree of decorrelation induced by NB stimulation. At the single unit level, although the between-cell CC was still reduced by NB stimulation, the magnitude of decorrelation was much smaller than that in the absence of atropine ($P < 10^{-28}$, Wilcoxon rank-sum test; n = 79 neurons from 12 experiments; Fig. 5b). Notably, atropine application was completely ineffective in blocking the NB-induced increase in response reliability. As quantified by the between-trial CC (Fig. 5c), NB stimulation induced a highly significant increase in reliability in the presence of atropine ($P < 10^{-13}$, Wilcoxon signed-rank test; n = 79 cells from 12 experiments). In fact, compared to the recordings in the absence of atropine (Fig. 4b), the NB-induced increase in reliability was slightly larger in the presence of atropine (Fig. 5c), although the difference was not statistically significant ($P = 0.08$, Wilcoxon rank-sum test).

Increased reliability involves distributed neural circuits

We also tested whether activation of nicotinic acetylcholine receptors (nAChRs) could underlie the increased response reliability, as they are known to enhance thalamocortical synaptic efficacy[25] and boost the visual responses of cortical neurons[30]. However, a marked NB-induced increase in response reliability was still present after cortical application of the selective nAChR antagonist mecamylamine [1 mM to 10 mM (surface application) or 100 μM to 1 mM (intracortical injection); $P < 10^{-12}$, Wilcoxon signed-rank test, n = 70 cells from 9 experiments] or Dihydro-β-erythroidine hydrobromide [DHβE, 100 μM (intracortical injection); $P < 0.001$, n = 16 cells from 3 experiments]. In the presence of these nAChR antagonists, the magnitude of the NB-induced increase was not reduced from that observed in the absence of the antagonists ($P = 0.97$, Wilcoxon rank-sum test). This suggests that NB stimulation may have altered the visual signals before they reached V1. To test this possibility, we made polytrode recordings in the lateral geniculate nucleus (LGN) of the thalamus (Fig. 6a). Indeed, single units in the LGN showed significant increases in response reliability following NB stimulation (Fig. 6b,c; $P < 10^{-12}$, Wilcoxon signed-rank test; n = 124 cells from 9 experiments), an effect that also remained highly significant after the spike rate equalization procedure ($P < 10^{-5}$, Wilcoxon signed-rank test). This may explain why cortical AChR antagonist application was ineffective in blocking the NB-induced increase in response reliability. Furthermore, NB stimulation caused a significant reduction of the ratio between burst and tonic spikes in LGN activity ($P < 10^{-10}$, Wilcoxon signed-rank test; Fig.

6d). This shift from burst to tonic firing mode has been shown to increase the linearity[39] and change the temporal response properties[40] of LGN neurons, which may further shape the input to the cortex. Thus, the NB-induced increase in response reliability is not a local effect in the cortex, but involves distributed neural circuits. Application of atropine (100 μM) and mecamylamine (100 μM) into the LGN (see Online Methods) did not block the NB-induced increase in cortical response reliability ($P < 10^{-7}$, $n = 42$ cells from 4 experiments, Supplementary Fig. 7 online), indicating that this effect is not mediated by cholinergic input to the LGN.

Decorrelation and increased repeatability improve coding

In principle, increased reliability and decreased correlation may improve visual coding by enhancing the coding capacity of each neuron and by reducing the redundancy between neurons, respectively[41]. To test this idea, we performed a simple discrimination analysis based on the V1 population responses to natural movies and compared the results before and after NB stimulation. For each pair of movie segments (100 ms per segment), we measured the discriminability of their responses by classifying the single-trial responses based on the similarity to each of the two template responses (mean responses across trials) (Fig. 7a; see Online Methods). We found that while the discrimination performance increased monotonically with the number of cells in the population (N), NB stimulation improved the performance at all N values tested ($P < 0.01$, Wilcoxon signed-rank test, with Bonferroni correction; 12 experiments; Fig. 7b).

To further investigate the effect of NB stimulation on visual coding, we evaluated the discrimination performance using an information theoretic measure (see Online Methods). Using single-neuron information, a measure unaffected by between-cell correlations, we found increased information after NB stimulation in all 19 experiments ($P < 0.001$, Wilcoxon signed-rank test; Fig. 7c). This is likely to reflect the contribution of increased response reliability of individual neurons. To test the effect of decorrelation on neural coding, we calculated the information ratio, defined as the total information from N cells [$I(N)$, $1 \leq N \leq 15$, averaged across all combinations of N cells in each recording] divided by the single-neuron information [$I(1)$, averaged across all single neurons in each recording]. For this measure (Fig. 7d), the ratio $I(N)/I(1)$ should be equal to N (diagonal line) if there is no redundancy between neurons. We found that in both control and NB conditions, the ratio was lower than N, reflecting redundancy between cells. However, the redundancy was significantly reduced by NB activation ($P < 0.05$ for $N = 7$ to 15 cells, Wilcoxon signed-rank test, with Bonferroni correction; 12 experiments). Thus, whereas the NB-induced improvement in response reliability increased the information coded by individual neurons (Fig. 7c), the decorrelation was associated with decreased redundancy among a population of neurons (Fig. 7d).

Discussion

Previous studies have shown that local application of ACh or AChR agonists can affect the firing rate and receptive field properties of visual cortical neurons[31–34,42], although the observed changes were diverse across neurons and sometimes inconsistent between studies.

In this study, by directly activating the source of cholinergic projections to the entire cortex, we have demonstrated two robust effects of NB activation on visual coding, mediated by distinct mechanisms. Furthermore, we found that both the decorrelation and increased reliability contribute to improved discriminability of the neuronal responses to different natural stimuli, a hallmark of enhanced visual coding.

In rat neocortex, nAChRs are expressed primarily in layer 4 (and to a lesser extent in layer 5) in both cortical neurons and thalamic terminals, whereas mAChRs (M_1–M_4) are expressed throughout the cortex, with different subtypes preferentially expressed in different layers[43]. Thalamocortical input is shown to be enhanced by nAChR activation, while excitatory intracortical synaptic activity can be suppressed by mAChRs[24,25]. The mAChR-mediated hyperpolarization of fast-spiking interneurons may also suppress thalamocortical feedforward inhibition[23,26]. Based on these effects at the cellular level, a common view is that ACh enhances thalamocortical inputs but suppresses intracortical interactions[24–27,44]. Our finding that NB-induced decorrelation between neurons requires local activation of mAChRs is consistent with this notion. However, while previous studies showed that activation of cortical AChRs increases the amplitude of thalamocortical input[30,45], we found that the improved response reliability was not reduced by local block of either mAChRs or nAChRs in the cortex (Fig. 5). This indicates that the NB-induced improvement in response reliability is not due primarily to the increased amplitude of thalamocortical input, but involves changes in the sensory signals earlier in the processing pathway. Our observation is also consistent with a recent finding that iontophoretic application of ACh in the visual cortex does not reduce the trial-to-trial variability of the neuronal responses[34].

Our experiments showed that NB stimulation increases the response reliability and decreases the burst-tonic ratio of LGN neurons (Fig. 6). Since NB does not project directly to the LGN, these effects must be mediated by indirect pathway(s) (through either cholinergic or GABAergic projections from the NB[46,47]), such as NB → cortex → LGN, NB → thalamic reticular nucleus → LGN[22,46], or NB → brainstem reticular formation → LGN[22,46] (although the lack of effect of atropine and mecamylamine injected into the LGN argues against the involvement of cholinergic projection from the reticular formation). These pathways could depolarize LGN neurons[29] and inactivate T-type Ca^{2+} channels[22,39], thereby increasing the response reliability and reducing the burst-tonic ratio. The changes in the LGN activity are likely to improve the fidelity of the sensory input to the cortex and thus explain the NB-induced increase in cortical response reliability (Fig. 4). Such distributed improvement of neuronal responses along the sensory pathway could contribute to NB-induced enhancement of sensory cortical plasticity[9,11], in addition to the local cholinergic effects in the cortex[10]. An intrinsic limitation of the extracellular stimulation technique is that it is difficult to distinguish the contributions of cholinergic and GABAergic NB neurons and to rule out the potential activation of axons originating from other brain regions passing through the NB. Future studies using optogenetic techniques[48] to activate specific cell types may help to determine the role of each cell type in regulating sensory coding along the thalamocortical pathway.

The activity of cholinergic neurons in the basal forebrain undergoes striking changes from the sleep to awake states[12,13,15]. Recent studies showed that even in the awake state NB

activity varies in a task-dependent manner[14,15], and it may be involved in regulating sensory processing under different forms of uncertainty[49]. Since NB receives input from both subcortical regions and prefrontal cortex[7], it may act as a way station for both bottom-up and top-down signals to regulate sensory coding in a behaviorally-relevant manner. Our finding that NB activation can rapidly improve visual representation in the cortex offers a mechanism by which perceptual abilities are enhanced during wakefulness, arousal, and attention.

Methods

Surgery

All experimental procedures were approved by the Animal Care and Use Committee at the University of California, Berkeley. Adult male Long-Evans rats (250–350 g) were anesthetized with urethane (i.p., 1.45 g kg^{-1}). Animals were restrained in a stereotaxic apparatus (David Kopf Instruments); body temperature was maintained at 37.5° C via a heating pad. Bipolar stimulating electrodes were stereotaxically implanted in the left nucleus basalis (NB), and NB was stimulated with trains of 50 pulses (0.1 ms $pulse^{-1}$) at 100 Hz. A craniotomy (diameter ~1 mm) was made either above the monocular region of left V1 or above the left LGN. A small portion of the dura was removed to allow insertion of a silicon polytrode (27 active channels separated by 50 μm, NeuroNexus Technologies). Signals were recorded with the Cheetah 32-channel acquisition system (Neuralynx) at 30 kHz. The right eye was fixed with a metal ring to prevent eye movement and irrigated with sterile saline. Following the experiment, animals were euthanized with an overdose of isoflurane. A total of 49 rats were used in this study.

Histochemistry

For histochemistry experiments, the animal was deeply anesthetized with urethane and immediately perfused with chilled 4% paraformaldehyde (PFA) solution in 0.1 M PBS. The brain was removed and fixed in 4% PFA/PBS solution overnight at 4° C. After fixation, the brain was sectioned into 150 μm horizontal slices using a vibratome (Serial 1000 Tissue Sectioning System, Ted Pella Inc). For acetylcholinesterase histochemistry, slices were incubated in 4 mM acetylcholine iodide, 4 mM copper sulphate, and 16 mM glycine in a 50 mM sodium acetate solution (pH 5.0) for 15 hr at 23° C and developed in 1% sodium sulphide solution (pH 7.0) for 10 min at 23° C. This procedure was performed in 15 of the 49 experiments included in this study.

Pharmacology

For topical drug application, a microwell was made by gluing a plastic ring to the skull surrounding the craniotomy. During application, antagonists to mAChRs (atropine, 1 mM) or nAChR (mecamylamine, 1–10 mM) were loaded into the microwell 15 min prior to recording. For intracortical injection, a glass micropipette (tip size ~10 μm) was fixed to the front of the polytrode such that the tip was close to the center of the polytrode recording sites (layer 4 or 5). Pharmacological antagonists to mAChRs (atropine, 100 μM) or nAChRs (mecamylamine, 100 μM – 1 mM; DHβE, 100 μM) were injected at a rate of 15 nl min^{-1} using a Hamilton syringe and a syringe pump, starting 15 min prior to and continuing

throughout the recording period (total volume ∼500 nl). Topical and intracortical pharmacology experiments were combined, since results were very similar for both methods.

To block LGN nAChRs and mAChRs (Supplementary Fig. 7 online), a mixture of 100 μM atropine and 100 μM mecamylamine was injected at 15 nl min^{-1} starting 15 min prior to and continuing throughout the recording. The volume of injection (∼500 nl) was determined in pilot experiments using dye injections to achieve coverage of most of the LGN without going much beyond its borders. To further ensure that the LGN neurons projecting to the recorded region of V1 were well exposed to the antagonists, we bonded a tungsten electrode to the injection pipette and mapped the LGN multiunit receptive field as closely as possible to the V1 multiunit receptive field.

Visual stimuli

Visual stimuli were generated with a PC computer containing a NVIDIA GeForce 6600 graphics board and presented with a XENARC 700V LCD monitor (19.7 cm × 12.1 cm, 960 × 600 pixels, 75 Hz refresh rate, 300 cd m^{-2} maximum luminance, gamma corrected with custom software) located 14 cm from the right eye, positioned such that the receptive fields of the recorded neurons were at the center of the monitor. For natural stimuli, three 5 s clips were selected from the van Hateren natural movie database. Each image (64 × 64 pixels, 36° × 36°, mean contrast 43%) was updated every 3 refresh frames, corresponding to an effective frame rate of 25 Hz. To avoid onset and offset transients, the first frame was displayed for 1 s prior to the movie and the last frame was displayed for 1 s following the movie.

Each experiment consisted of 6 blocks, and each block consisted of 5 repeats of the three movies under control and 5 repeats under NB conditions (Supplementary Fig. 4a online). Under the control condition, the movies were repeated 5 times with 2 s of static image before each movie. Under the NB condition, the movies were repeated 5 times as in the control condition, and NB stimulation was administered from 1000 ms to 500 ms prior to the start of each movie. To ensure that the effect of NB stimulation had diminished before the start of control trials, a blank frame was shown for 30 s following each block. Each experiment thus consisted of 30 movie repeats under control and 30 repeats under NB conditions. In blocks 1 to 3, the control repeats preceded the NB repeats; in blocks 4 to 6, the sequence was reversed to further eliminate the potential effect of stimulus history on cortical responses.

For measuring receptive fields (Supplementary Fig. 5 online), sparse noise consisting of random flashes of white and black pixels (100% contrast, 4.5° $pixel^{-1}$, 100 ms per flash) on a gray background was used. For measuring orientation tuning and direction selectivity (Supplementary Fig. 6 online), drifting gratings (100% contrast, 2 Hz, 0.04 cycles deg^{-1})were used.

Analyses

Local field potential analysis was carried out using Gabor/Morlet wavelet decomposition (http://dxjones.com/matlab/timefreq/). For single unit isolation, polytrode contact sites

(channels) were separated into groups (2–4 channels per group) and spike waveforms were sorted using NeuroScope (http://neuroscope.sourceforge.net), NDManager (http://ndmanager.sourceforge.net), and Klusters (http://klusters.sourceforge.net)[50]. In some instances, a single neuron was picked up by more than one electrode group. To ensure that duplicate neurons were not included in the subsequent analyses, pairwise between-neuron correlation coefficients (CC; binned at 1000 Hz) were calculated following clustering; for any pair with CC > 0.1, the cell with lower firing rate was discarded. For the remaining single units, only those with firing rates > 0.5 spikes s^{-1} were included in further analyses, performed in MATLAB (The Mathworks).

For calculation of between-cell and between-trial CC (Figs. 2 and 3), firing rates were binned at 10 Hz (although results were similar for binning from 5 Hz to 25 Hz). To determine whether a given cell was visually driven, we compared the average between-trial CC within movies and between movies. Only cells that had significantly higher within-movie CC (threshold $\alpha = 0.01$, Wilcoxon signed-rank test) were included in further analyses. The burst-tonic ratio was calculated by measuring the number of burst spikes (two or more spikes occurring with ISI < 4 ms following an absence of spiking for > 100 ms) relative to the number of tonic spikes (all spikes not meeting the burst criteria).

To quantify the ON and OFF receptive fields measured with sparse noise (Supplementary Fig. 5 online), each receptive field was fitted with a two-dimensional Gaussian function:

$$R(x,y) = a_0 + ae^{-\left(\frac{(x-x_0)^2}{2\sigma_M^2} + \frac{(y-y_0)^2}{2\sigma_m^2}\right)}$$

where $R(x,y)$ is the response at pixel position (x,y), a_0 is the DC component, a is the receptive field peak amplitude, (x_0,y_0) is the receptive field center, and σ_M and σ_m are the standard deviations along the major and minor axes. The receptive field size is measured by $\pi\sigma_M\sigma_m$, and the amplitude/baseline ratio is measured by a/a_0.

To measure orientation tuning and direction selectivity (Supplementary Fig. 6 online), firing rate as a function of orientation was fitted as the sum of two Gaussians with peaks 180° apart:

$$R(\theta) = a_0 + a_1 e^{\frac{-(\theta-\theta_0)^2}{2\sigma^2}} + a_2 e^{\frac{-\left(\theta-\theta_0+180^\circ\right)^2}{2\sigma^2}}$$

where $R(\theta)$ is the response at orientation θ, a_0 is the DC component, a_1 and a_2 are the amplitudes of the two Gaussians, θ_0 is the preferred orientation, and σ is the standard deviation. Tuning width is measured by σ, and direction selectivity is measured by $[R(\theta_0)-R(\theta_0+180°)]/[R(\theta_0)+R(\theta_0+180°)]$.

For the discrimination analysis (Fig. 7), the responses were also binned at 10 Hz. For each discrimination, the single-trial response in a given bin (A_i, where i is the trial number) was

compared to the mean responses (averaged across trials) in the same bin (<*A*>) and in a different bin (<*B*>) based on the Euclidian distances $d(A_i, \langle A \rangle)$ and $d(A_i, \langle B \rangle)$. The classification was considered correct if $d(A_i, \langle A \rangle) < d(A_i, \langle B \rangle)$, and incorrect if $d(A_i, \langle A \rangle) > d(A_i, \langle B \rangle)$. Discrimination performance was assessed by the percentage of correct classifications for all the trials. Since the discrimination performance is expected to increase nonlinearly with the number of neurons, it is difficult to measure the redundancy between neurons. We thus converted the discrimination performance into a measure of information as $I = 1 + (p)\log_2(p) + (1-p)\log_2(1-p))$, where p is the discrimination performance (note that when discrimination is at chance level, $p = 50\%$, $I = 0$). This definition of I represents the mutual information between the actual stimulus and the stimulus decoded from the neuronal response by the 'ideal observer' in the discrimination analysis. $I(N)$ is computed as the average information across all combinations of N simultaneously recorded cells in each experiment, and it should increase linearly with N if there is no redundancy between neurons. Downward deviation from the diagonal line in Fig. 7d thus reflects the degree of redundancy. For population analyses (Fig. 7b,d), only experiments with ≥ 15 simultaneously recorded single units were included (12/19 experiments).

To test statistical significance, Wilcoxon signed-rank test was used for paired samples and Wilcoxon rank-sum test was used for unpaired samples; multiple comparisons were corrected with the Bonferroni method.

Supplementary Material

Refer to Web version on PubMed Central for supplementary material.

Acknowledgments

This work was supported by grants from the US National Institutes of Health to Y.D., and a Ruth L. Kirschstein National Research Service Award to M.G. (Award Number F31NS059258 from the US National Institute of Neurological Disorders and Stroke). We thank T. Blanche, D. Feldman, R. Froemke, D. Jones, D. Kleinfeld, C. Niell, and A. Vahidnia for technical help and useful discussions.

References

1. Robbins TW. Arousal systems and attentional processes. Biol Psychol. 1997; 45:57–71. [PubMed: 9083644]
2. Jones BE. Modulation of cortical activation and behavioral arousal by cholinergic and orexinergic systems. Ann N Y Acad Sci. 2008; 1129:26–34. [PubMed: 18591466]
3. Berridge CW, Waterhouse BD. The locus coeruleus-noradrenergic system: modulation of behavioral state and state-dependent cognitive processes. Brain Res Brain Res Rev. 2003; 42:33–84. [PubMed: 12668290]
4. Steriade, M.; McCarley, RW. Brainstem control of wakefulness and sleep. Plenum Press; New York: 1990.
5. Lehmann J, Nagy JI, Atmadia S, Fibiger HC. The nucleus basalis magnocellularis: the origin of a cholinergic projection to the neocortex of the rat. Neuroscience. 1980; 5:1161–74. [PubMed: 7402465]
6. Everitt BJ, Robbins TW. Central cholinergic systems and cognition. Annu Rev Psychol. 1997; 48:649–84. [PubMed: 9046571]

7. Sarter M, Hasselmo ME, Bruno JP, Givens B. Unraveling the attentional functions of cortical cholinergic inputs: interactions between signal-driven and cognitive modulation of signal detection. Brain Res Brain Res Rev. 2005; 48:98–111. [PubMed: 15708630]
8. Hasselmo ME. Neuromodulation and cortical function: modeling the physiological basis of behavior. Behav Brain Res. 1995; 67:1–27. [PubMed: 7748496]
9. Kilgard MP, Merzenich MM. Cortical map reorganization enabled by nucleus basalis activity. Science. 1998; 279:1714–8. [PubMed: 9497289]
10. Froemke RC, Merzenich MM, Schreiner CE. A synaptic memory trace for cortical receptive field plasticity. Nature. 2007; 450:425–9. [PubMed: 18004384]
11. Bakin JS, Weinberger NM. Induction of a physiological memory in the cerebral cortex by stimulation of the nucleus basalis. Proc Natl Acad Sci U S A. 1996; 93:11219–24. [PubMed: 8855336]
12. Lee MG, Hassani OK, Alonso A, Jones BE. Cholinergic basal forebrain neurons burst with theta during waking and paradoxical sleep. J Neurosci. 2005; 25:4365–9. [PubMed: 15858062]
13. Jones BE. Activity, modulation and role of basal forebrain cholinergic neurons innervating the cerebral cortex. Prog Brain Res. 2004; 145:157–69. [PubMed: 14650914]
14. Laplante F, Morin Y, Quirion R, Vaucher E. Acetylcholine release is elicited in the visual cortex, but not in the prefrontal cortex, by patterned visual stimulation: a dual in vivo microdialysis study with functional correlates in the rat brain. Neuroscience. 2005; 132:501–10. [PubMed: 15802200]
15. Parikh V, Kozak R, Martinez V, Sarter M. Prefrontal acetylcholine release controls cue detection on multiple timescales. Neuron. 2007; 56:141–54. [PubMed: 17920021]
16. Fiser J, Chiu C, Weliky M. Small modulation of ongoing cortical dynamics by sensory input during natural vision. Nature. 2004; 431:573–578. [PubMed: 15457262]
17. Tsodyks M, Kenet T, Grinvald A, Arieli A. Linking spontaneous activity of single cortical neurons and the underlying functional architecture. Science. 1999; 286:1943–1946. [PubMed: 10583955]
18. Poulet JF, Petersen CC. Internal brain state regulates membrane potential synchrony in barrel cortex of behaving mice. Nature. 2008; 454:881–5. [PubMed: 18633351]
19. Petersen CC, Hahn TT, Mehta M, Grinvald A, Sakmann B. Interaction of sensory responses with spontaneous depolarization in layer 2/3 barrel cortex. Proc Natl Acad Sci U S A. 2003; 100:13638–43. [PubMed: 14595013]
20. Worgotter F, et al. State-dependent receptive-field restructuring in the visual cortex. Nature. 1998; 396:165–8. [PubMed: 9823895]
21. Metherate R, Cox CL, Ashe JH. Cellular bases of neocortical activation: modulation of neural oscillations by the nucleus basalis and endogenous acetylcholine. J Neurosci. 1992; 12:4701–11. [PubMed: 1361197]
22. McCormick DA. Neurotransmitter actions in the thalamus and cerebral cortex and their role in neuromodulation of thalamocortical activity. Prog Neurobiol. 1992; 39:337–88. [PubMed: 1354387]
23. Xiang Z, Huguenard JR, Prince DA. Cholinergic switching within neocortical inhibitory networks. Science. 1998; 281:985–8. [PubMed: 9703513]
24. Hsieh CY, Cruikshank SJ, Metherate R. Differential modulation of auditory thalamocortical and intracortical synaptic transmission by cholinergic agonist. Brain Res. 2000; 880:51–64. [PubMed: 11032989]
25. Gil Z, Connors BW, Amitai Y. Differential regulation of neocortical synapses by neuromodulators and activity. Neuron. 1997; 19:679–86. [PubMed: 9331357]
26. Kruglikov I, Rudy B. Perisomatic GABA release and thalamocortical integration onto neocortical excitatory cells are regulated by neuromodulators. Neuron. 2008; 58:911–24. [PubMed: 18579081]
27. Oldford E, Castro-Alamancos MA. Input-specific effects of acetylcholine on sensory and intracortical evoked responses in the “barrel cortex” in vivo. Neuroscience. 2003; 117:769–78. [PubMed: 12617980]
28. Bazhenov M, Timofeev I, Steriade M, Sejnowski TJ. Model of thalamocortical slow-wave sleep oscillations and transitions to activated States. J Neurosci. 2002; 22:8691–704. [PubMed: 12351744]

29. Castro-Alamancos MA. Dynamics of sensory thalamocortical synaptic networks during information processing states. Prog Neurobiol. 2004; 74:213–47. [PubMed: 15556288]
30. Disney AA, Aoki C, Hawken MJ. Gain modulation by nicotine in macaque v1. Neuron. 2007; 56:701–13. [PubMed: 18031686]
31. Sillito AM, Kemp JA. Cholinergic modulation of the functional organization of the cat visual cortex. Brain Res. 1983; 289:143–55. [PubMed: 6661640]
32. Muller CM, Singer W. Acetylcholine-induced inhibition in the cat visual cortex is mediated b7 a GABAergic mechanism. Brain Res. 1989; 487:335–42. [PubMed: 2731048]
33. Sato H, Hata Y, Masui H, Tsumoto T. A functional role of cholinergic innervation to neurons in the cat visual cortex. J Neurophysiol. 1987; 58:765–80. [PubMed: 3681394]
34. Zinke W, et al. Cholinergic modulation of response properties and orientation tuning of neurons in primary visual cortex of anaesthetized Marmoset monkeys. Eur J Neurosci. 2006; 24:314–28. [PubMed: 16882027]
35. Herrero JL, et al. Acetylcholine contributes through muscarinic receptors to attentional modulation in V1. Nature. 2008; 454:1110–4. [PubMed: 18633352]
36. Buzsaki G, et al. Nucleus basalis and thalamic control of neocortical activity in the freely moving rat. J Neurosci. 1988; 8:4007–26. [PubMed: 3183710]
37. Blanche TJ, Spacek MA, Hetke JF, Swindale NV. Polytrodes: high-density silicon electrode arrays for large-scale multiunit recording. J Neurophysiol. 2005; 93:2987–3000. [PubMed: 15548620]
38. Paxinos, G.; Watson, C. The rat brain in stereotaxic coordinates. Academic Press; San Diego: 1998.
39. Sherman SM. Dual response modes in lateral geniculate neurons: mechanisms and functions. Vis Neurosci. 1996; 13:205–13. [PubMed: 8737271]
40. Bezdudnaya T, et al. Thalamic burst mode and inattention in the awake LGNd. Neuron. 2006; 49:421–32. [PubMed: 16446145]
41. Barlow H. Redundancy reduction revisited. Network. 2001; 12:241–53. [PubMed: 11563528]
42. Roberts MJ, et al. Acetylcholine dynamically controls spatial integration in marmoset primary visual cortex. J Neurophysiol. 2005; 93:2062–72. [PubMed: 15548624]
43. Zilles K, et al. Distribution of cholinergic receptors in the rat and human neocortex. Exs. 1989; 57:212–28. [PubMed: 2558907]
44. Kimura F, Fukuda M, Tsumoto T. Acetylcholine suppresses the spread of excitation in the visual cortex revealed by optical recording: possible differential effect depending on the source of input. Eur J Neurosci. 1999; 11:3597–609. [PubMed: 10564367]
45. Metherate R, Ashe JH. Nucleus basalis stimulation facilitates thalamocortical synaptic transmission in the rat auditory cortex. Synapse. 1993; 14:132–43. [PubMed: 8392756]
46. Parent A, Pare D, Smith Y, Steriade M. Basal forebrain cholinergic and noncholinergic projections to the thalamus and brainstem in cats and monkeys. J Comp Neurol. 1988; 277:281–301. [PubMed: 2466060]
47. Lin SC, Gervasoni D, Nicolelis MA. Fast modulation of prefrontal cortex activity by basal forebrain noncholinergic neuronal ensembles. J Neurophysiol. 2006; 96:3209–19. [PubMed: 16928796]
48. Zhang F, Aravanis AM, Adamantidis A, de Lecea L, Deisseroth K. Circuit-breakers: optical technologies for probing neural signals and systems. Nat Rev Neurosci. 2007; 8:577–81. [PubMed: 17643087]
49. Yu AJ, Dayan P. Uncertainty, neuromodulation, and attention. Neuron. 2005; 46:681–92. [PubMed: 15944135]
50. Hazan L, Zugaro M, Buzsaki G. Klusters, NeuroScope, NDManager: a free software suite for neurophysiological data processing and visualization. J Neurosci Methods. 2006; 155:207–16. [PubMed: 16580733]

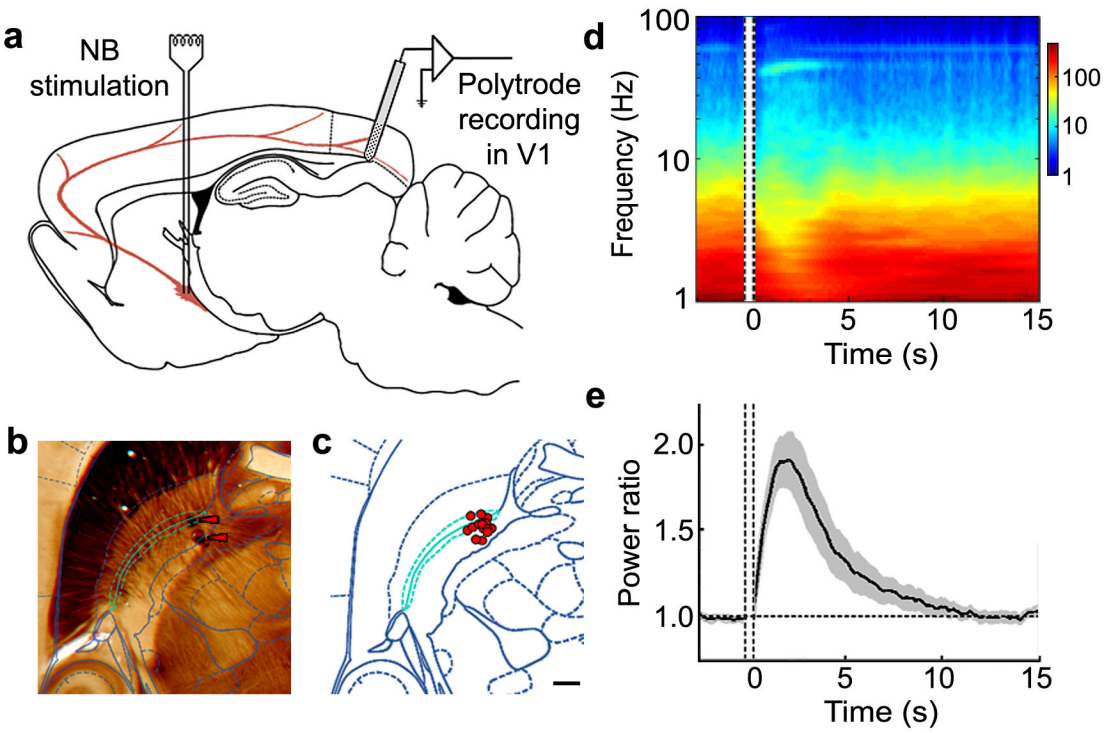

Figure 1.

Effects of NB stimulation on local field activity in V1. (**a**) Schematic illustration of experimental setup, adapted from Paxinos and Watson rat brain atlas[38]. (**b**) An example of stimulation electrode localization using acetylcholinesterase histochemistry. NB is shown in cyan in overlay diagram (from Paxinos and Watson atlas[38]). Red arrowheads, bipolar electrode tracts. (**c**) Summary of electrode positions relative to NB (cyan) for 15 experiments. Red circle, centroid of the pair of electrode tracts in each experiment, which was within 300 μm of NB for all 15 experiments. Scale bar, 500 μm. (**d**) Time-frequency analysis of LFP before and after NB stimulation from an example experiment, averaged over 30 trials. Amplitude is color coded (scale bar on the right, arbitrary unit). Vertical lines, period of NB stimulation (500 ms). No visual stimuli were presented. (**e**) Power ratio (LFP power at 10 to 100 Hz divided by LFP power at 1 to 10 Hz) averaged across 27 experiments. In each experiment the ratio was normalized by its mean value before NB stimulation. Black line, mean; shaded area, ± s.e.m.

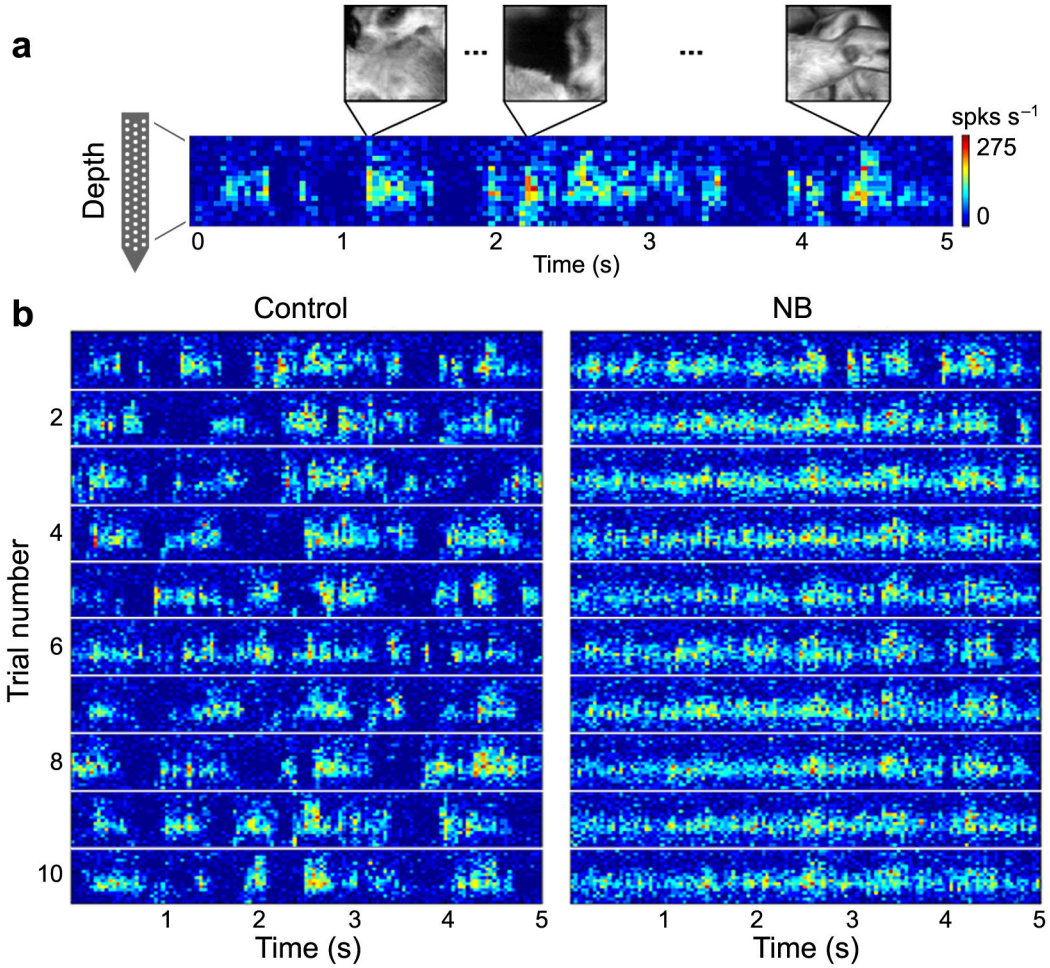

Figure 2.

Effect of NB stimulation on multiunit activity throughout the depth of cortex. (**a**) Multiunit spike rate (color coded, scale bar on the right) recorded by the polytrode plotted against cortical depth and time during one repeat of a natural movie (only 18 of the 27 polytrode channels are shown). (**b**) Multiunit responses to the first 10 repeats (trials) of the movie, before (control) and 0 to 5 s after NB stimulation, both plotted on the color scale shown in (**a**).

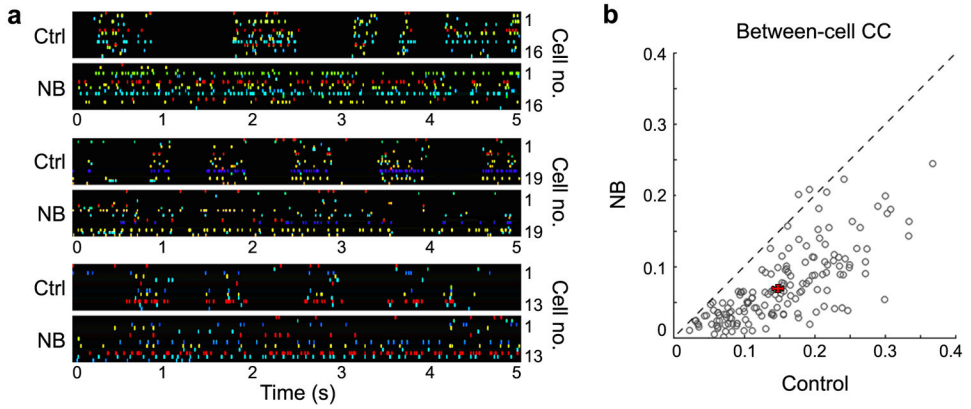

Figure 3.

NB stimulation decreases correlation between cortical neurons during visual stimulation. (**a**) Three example experiments illustrating changes in between-cell correlation before (Ctrl) and after (NB) basal forebrain activation. Each panel shows the responses of multiple single units recorded simultaneously during a single movie repeat. Different neurons are indicated by different colors and ordered by cortical depth. (**b**) Summary of between-cell CC before and after NB stimulation (n = 166 cells from 19 experiments). Each circle represents the average CC between a single neuron and all other neurons in the same recording. Error bars, ± s.e.m.

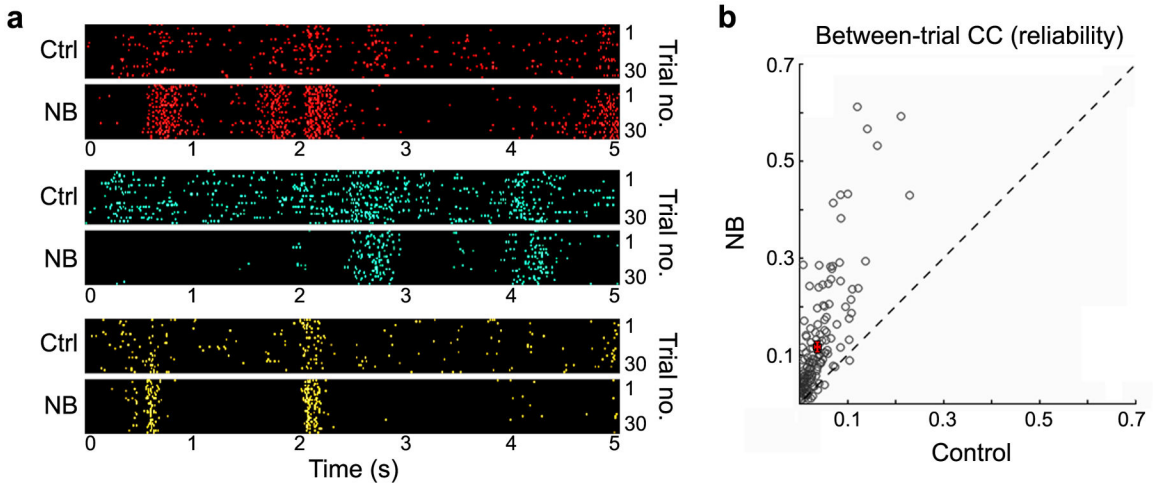

Figure 4.

NB stimulation increases reliability of individual neurons in response to natural scenes. (**a**) Three example neurons (indicated by different colors) illustrating changes in response reliability before (Ctrl) and after (NB) basal forebrain activation. Each panel shows the responses of a single neuron to 30 repeats (trials) of a movie. (**b**) Summary of response reliability measured by between-trial CC before and after NB stimulation (166 cells from 19 experiments). Each circle represents data from one neuron, averaged over CCs for all pairwise combinations of the 30 trials. Error bars, ± s.e.m.

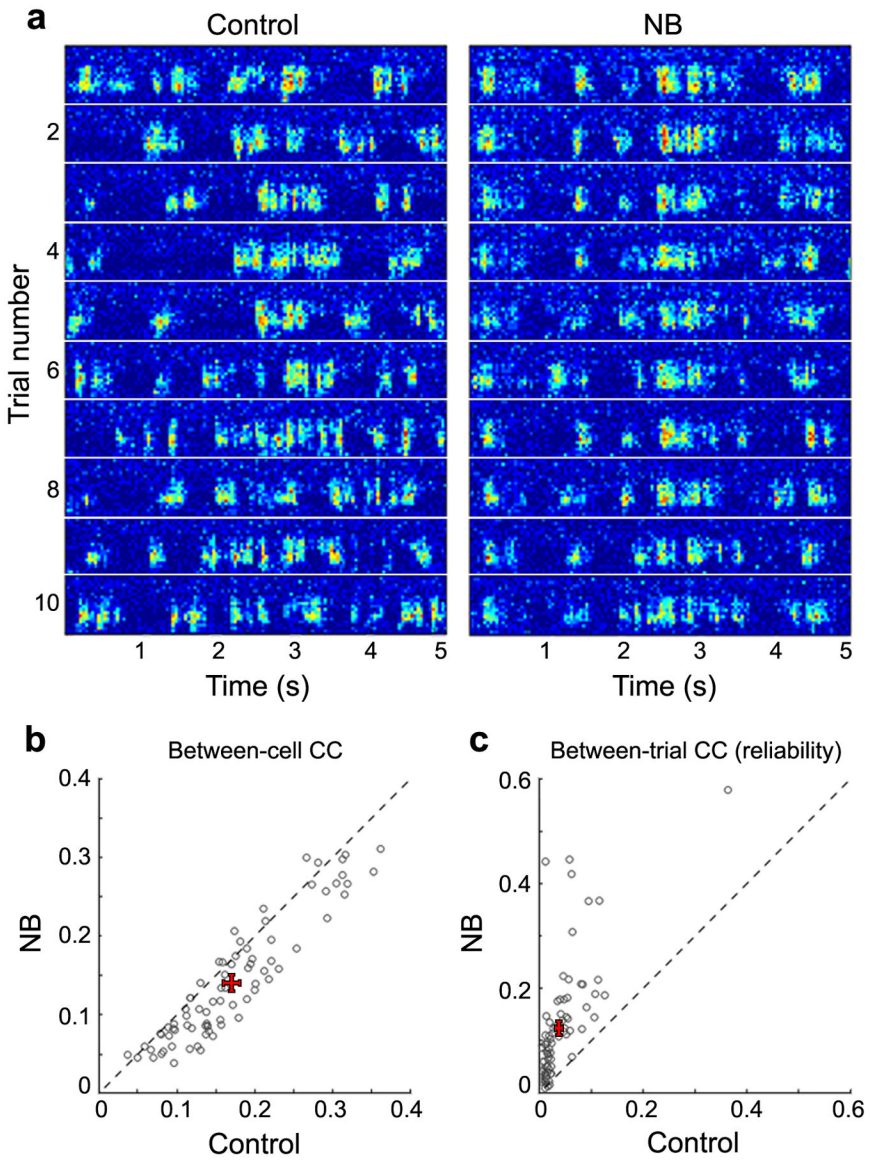

Figure 5.

Application of mAChR antagonist diminishes NB-induced decorrelation but does not affect increases in response reliability. (**a**) An example of multiunit responses to the first 10 repeats of a movie before (Control) and after (NB) basal forebrain activation in the presence of atropine (100 μM, intracortical injection). Note that the correlation between channels was strong in both Control and NB conditions, but the response was much more time-locked to the movie after NB stimulation. (**b**) Summary of between-cell CC before (Control) and after NB stimulation in the presence of atropine (n = 79 single units from 12 experiments). (**c**) Summary of between-trial CC before (Control) and after NB stimulation in the presence of atropine (n = 79 single units from 12 experiments).

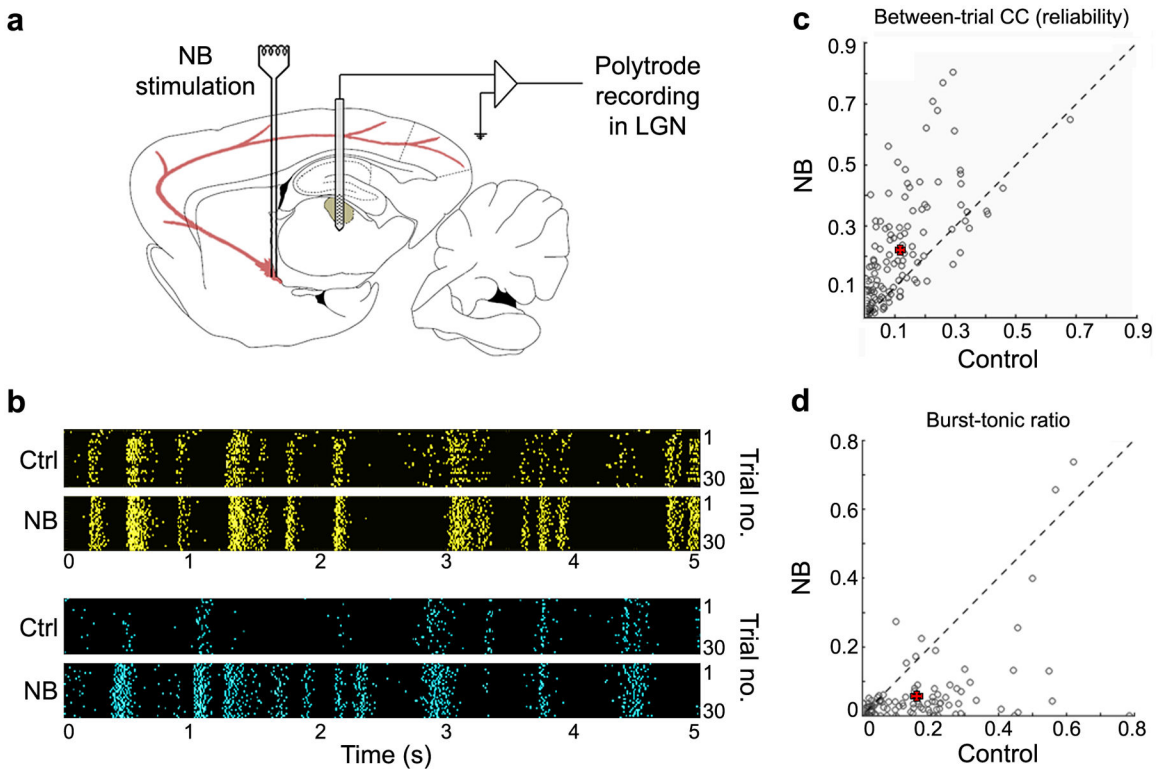

Figure 6.

NB stimulation increases response reliability and shifts firing mode in the LGN. (**a**) Schematic illustration of experimental setup. (**b**) Responses of two example LGN single units before (Ctrl) and after NB stimulation. Each panel shows the responses to 30 repeats of a movie. (**c**) Between-trial CC before (Control) and after NB stimulation (n = 124 cells from 9 experiments). (**d**) Burst-tonic ratio of LGN neurons before (Control) and after NB stimulation in the absence of visual stimulus. Each circle represents the burst-tonic ratio of one LGN neuron (n = 105 cells from 3 experiments). Error bars, ± s.e.m.

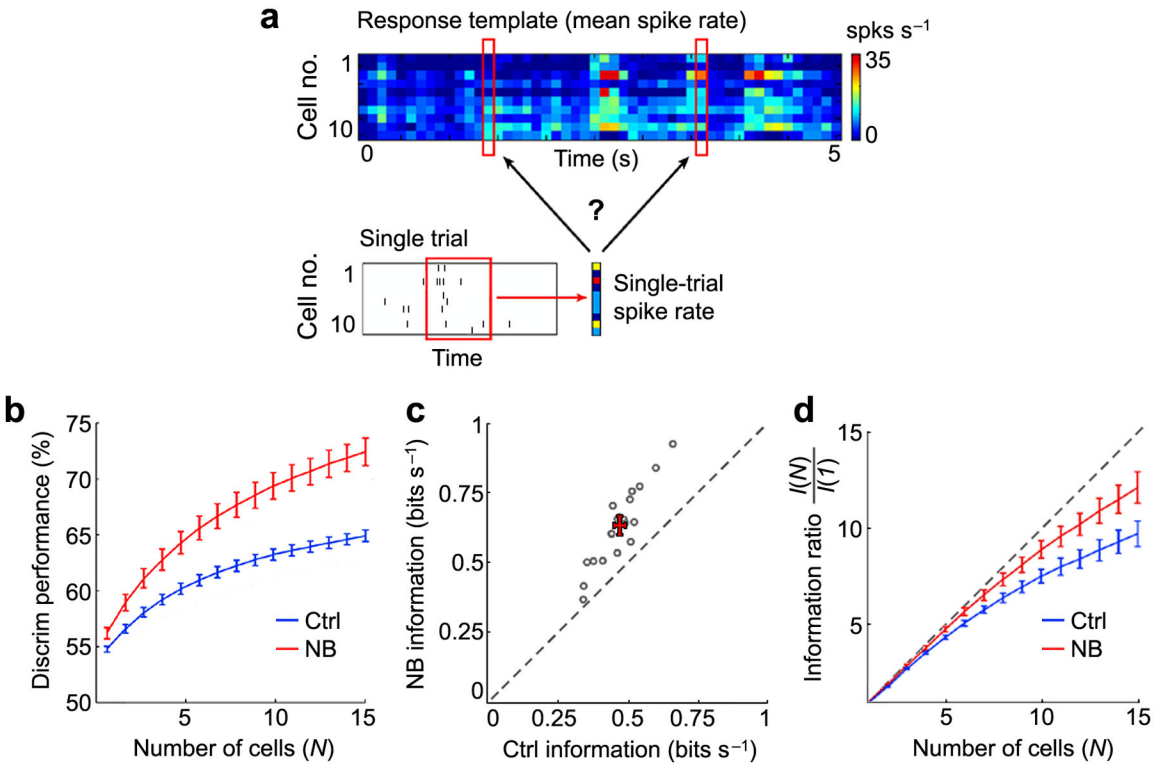

Figure 7.

Increased reliability and decreased correlation both contribute to improved coding of natural stimuli. (**a**) Schematic illustration of the discrimination analysis. The population response during a given stimulus segment (100 ms, red box) in each trial was classified as one of two categories based on its Euclidean distances from the two templates (population responses averaged across trials). (**b**) Mean discrimination performance (% of correct classifications) as a function cell number (*N*) included in the population analysis for control and NB conditions (12 experiments). (**c**) Single-neuron information [*I*(1)] before and after NB stimulation. Each point represents *I*(1) averaged across all cells in each experiment (19 experiments). (**d**) Information ratio [*I*(*N*)/*I*(1)] as a function of cell number (*N*) before and after NB stimulation (12 experiments). Diagonal line indicates linear summation of information (no redundancy between cells). Error bars, ± s.e.m.